ELSEVIER SCIENCE Ltd. [DTD 4.1.0]
JOURNAL CHEGLO ARTICLE No. 109
PAGES 1-10 DISPATCH 30 December 2000 PROD. TYPE: FROM DISK
CHEGLO 109
A

PERGAMON

Chemosphere – Global Change Science 000 (2000) 000–000

CHEMOSPHERE – GLOBAL CHANGE SCIENCE

The sensitivity of tropospheric methane to the interannual variability in stratospheric ozone

Charles D. Camp [a,*], Mark S. Roulston [b], Albert F.C. Haldemann [c], L. Yung [d]

[a] *Department of Applied Mathematics, California Institute of Technology, Pasadena, CA 91125, USA*
[b] *Pembroke College, Oxford, OX1 1DW, UK*
[c] *Jet Propulsion Laboratory, California Institute of Technology, Pasadena, CA 91125, USA*
[d] *Division of Geological and Planetary Sciences, California Institute of Technology, Pasadena, CA 91125, USA*

Received 25 April 2000; received in revised form 8 August 2000; accepted 12 September 2000

Importance of this paper: Many processes in the stratosphere have important impacts upon tropospheric behavior. The forcing of tropospheric methane by stratospheric ozone is one such interaction for which we have long and accurate observational records. We have empirically determined a quantitative measure of this interaction. This result provides the first convincing demonstration in the data records of such a stratosphere–troposphere interaction. It can also be used to calibrate the modeling work being done in this area.

Abstract

The dominant processes affecting the concentration of tropospheric methane on interannual timescales are the biospheric and anthropogenic sources and changes in the abundance of the hydroxyl radical caused by the changes in the UV flux which result from changes in stratospheric ozone abundance. We have carried out an empirical study of the sensitivity of the methane to fluctuations in ozone column abundance. This analysis was carried out using monthly mean surface methane concentrations measured by the National Oceanic and Atmospheric Administration – Climate Monitoring and Diagnostics Laboratory (NOAA-CMDL) Global Cooperative Air Sampling Network from 1983 to 1998 and ozone column abundances obtained by the Total Ozone Mapping Spectrometer (TOMS) and the EP TOMS instruments over the same time period. We focused on interannual variability with periods between 15 and 60 months, in which interval the dominant ozone fluctuation is the quasi-biennial oscillation (QBO), with a period of approximately 29 months. In order to isolate the response of methane to ozone from the effects of variability in the sources and transport of methane, we restricted our analysis to data at mid-latitudes in the southern hemisphere. A statistical study shows that the sensitivity factor $\alpha \equiv -d(\ln[CH_4])/d(\ln[O_3]) = -0.038 \pm 0.009$. The response of CH_4 lags approximately 6 months behind the forcing by O_3. A simple model was used to interpret the empirical results. Our results confirm that any mechanism that affects stratospheric ozone impacts the oxidizing potential of the troposphere. CH_4 fluctuations provide a quantitative measure of this important effect linking the upper and the lower atmosphere.

Keywords: Interannual oscillation; QBO; Atmosphere; Stratosphere–troposphere interaction; Insolation

1. Introduction

The most important mechanism for removing methane from the atmosphere is its reaction with tropospheric OH radicals (Khalil et al., 1993).

* Corresponding author. Tel.: +1-626-395-3992; fax: +1-626-585-1917.
E-mail address: cdc@gps.caltech.edu (C.D. Camp).

1465-9972/00/$ - see front matter
PII: S1465-9972(00)00053-2

$$CH_4 + OH \rightarrow CH_3 + H_2O. \quad (1)$$

The primary source of OH is the UV photolysis of tropospheric ozone to give electronically excited oxygen atoms. A small fraction of these excited atoms then react with water to produce the OH radical. This source of OH is described by

$$O_3 + h\nu \rightarrow O(^1D) + O_2, \quad (2)$$

$$O(^1D) + H_2O \rightarrow 2OH, \quad (3)$$

where $h\nu$ is a near-UV photon (Levy, 1992, Thompson, 1992). As oxidation by OH is the main loss mechanism for tropospheric methane it follows that any perturbation to the abundance of OH will affect the abundance of methane. Any modulation of the UV flux to the troposphere will affect the abundance of OH (Liu and Tranier, 1988), which will in turn modulate the concentration of methane via reactions (1)–(3). The primary source of UV fluctuations on interannual timescales is fluctuations in the ozone column abundance.

For small perturbations, these effects may be approximated by the linear relations

$$\frac{[OH]'}{[OH]_0} = -\alpha_{OH}\frac{\Omega'}{\Omega_0}, \quad (4)$$

$$\frac{[CH_4]'}{[CH_4]_0} = -\alpha_{CH_4}\frac{\Omega'}{\Omega_0}, \quad (5)$$

where α is the sensitivity of a given species to changes in the ozone column abundance. Ω_0 and Ω' are, respectively, the reference level and the perturbation from the reference level of ozone, with similar definitions for reference levels and perturbations of the concentrations of CH_4 and OH. The minus sign follows the convention in the literature (Fuglestvedt et al., 1994, Granier and Shine, 1991). We expect α_{CH_4} to be negative, since the oscillations in methane are positively correlated with the oscillations in ozone. A value for α_{CH_4} can be calculated from a comparison of the observations of the fluctuations in the methane signal to those in the ozone signal. Note that the α so determined is based on the methane's relatively short response time to the ozone oscillations and is therefore fundamentally different from the α's obtained from studies using models run until a steady state is achieved (Bekki et al., 1994; Fuglestvedt et al., 1994; Granier et al., 1996; Van Dop and Krol, 1996). However, the empirically determined α can, with appropriate modifications, still be used to calibrate the behavior of the modeling studies. This is explored in more detail in Sections 2 and 4.

While the sensitivity will be determined empirically, a simple model can be used to help interpret the results. Changes in methane concentration can be modeled by the equation

$$\frac{d[CH_4]}{dt} = P - k[OH][CH_4], \quad (6)$$

where P is the production of methane and k is the rate coefficient for destruction of methane by OH. P and k are assumed to be constants. The methane concentration can be written as $[CH_4] = [CH_4]_0 + [CH_4]'$ and the OH concentration as $[OH] = [OH]_0 + [OH]'$, where a zero subscript represents the time-invariant mean and a prime represents the deviation from the mean. Eq. (6) can now be expanded

$$\frac{d[CH_4]'}{dt} = P - k[OH]_0[CH_4]_0 - k[OH]_0[CH_4]' - k[OH]'[CH_4]_0 - k[OH]'[CH_4]'. \quad (7)$$

The first two terms on the right-hand side of (7) cancel since the steady-state solution of (6) gives $P - k[OH]_0[CH_4]_0 = 0$. The last term is second-order in the perturbation and can be neglected for small perturbations. Dividing the remaining terms in (7) by $[CH_4]_0$ leaves the linearized model

$$\frac{dy}{dt} = -\frac{y}{\tau} - \frac{F(t)}{\tau}, \quad (8)$$

where $y = [CH_4]'/[CH_4]_0$ is the fractional deviation from the mean methane concentration and $F = [OH]'/[OH]_0$ is the fractional deviation of the OH concentration. $\tau = 1/k[OH]_0$ is the mean lifetime of methane in the troposphere. This analysis can be expanded to a time-dependent source, $P(t)$, by detrending the chemical time series and assuming that $P(t)$ balances the trends removed. Since the lifetime of OH in the atmosphere is extremely short, the perturbations in OH should very closely track the perturbations in O_3. For small perturbations, the forcing term in Eq. (8) can be represented as

$$F(t) = \kappa\frac{\Omega'}{\Omega_0}, \quad (9)$$

where, as before, Ω represents the total column abundance of ozone. The constant of proportionality, κ, is closely related to the sensitivity, α. The exact relationship between κ and α is examined in Section 3 and in Appendix A.

2. Sensitivity to interannual fluctuations

We have carried out an empirical study of the sensitivity of the methane to interannual fluctuations in ozone column abundance. The ozone data set we used was one of the merged ozone data sets (MOD) which combine the monthly mean column abundances collected by the Total Ozone Mapping Spectrometer (TOMS) instruments on Nimbus-7, Meteor-3 and Earth Probe with the total ozone measurements collected by the Solar Backscatter Ultraviolet (SBUV/SBUV2) instruments on Nimbus 7, NOAA 9 and NOAA 11 (McPeters et al., 1996; Bojkov and Hudson, 1991). We

used version 1, all stations, of the combined data set (SBUV + TOMS), as described in the NASA web site: http://hyperion.gsfc.nasa.gov/Analysis/merged. The methane data we used were monthly means of surface methane measurements made from samples collected at fixed sites in the National Oceanic and Atmospheric Administration – Climate Monitoring and Diagnostics Laboratory (NOAA-CMDL) Global Cooperative Air Sampling Network (Dlugokency et al., 1997). These samples are taken at approximately weekly intervals.

We restricted our analysis to data at mid-latitudes in the southern hemisphere. In the northern hemisphere, fluctuations in the methane production by the terrestrial biosphere and by anthropogenic sources obscure the weak signal in the data. In the tropics, CH_4 is transported from mid-latitudes by the convergence of surface winds near the equator, introducing additional fluctuations other than those caused by stratospheric O_3. In our analysis, we used the Cape Grim (CGO) (40°41′S, 144°41′E) site from the NOAA-CMDL methane data set. Of the southern sites, CGO is the only site with a long continuous record that is also remote from known sources of methane. For ozone, we used the [40°S, 45°S] latitude band of the TOMS ozone data set. We had ozone data for the months from November 1978 to March 1999, but we had methane data only for the months from April 1984 to December 1998. Therefore our calculation of the sensitivity was done using the latter time domain where we had data for both ozone and methane.

Both data sets were quadratically detrended and then their seasonal cycles were removed. Missing months were interpolated using cubic splines. Further filtering was done spectrally to isolate fluctuations with periods between 15 and 60 months. The spectral filter was a convolution of stepfunctions with Hanning windows chosen to get a full signal from periods inside the (15, 60) month interval and no signal from periods outside of the (12.5, 92) month interval (Press et al., 1992a). The frequency filtering was done to remove those periods for which the changes in the UV flux to the troposphere are not simply the result of changes in stratospheric ozone. For the seasonal cycle (and shorter periods) the fluctuations in UV insolation annual cycle are large, of roughly the same order as the mean values. The reason for removing the longer period fluctuations was to eliminate the solar cycle. The solar cycle manifests itself both as a change in the UV insolation to the top of the atmosphere and an associated change in stratospheric ozone which in turn leads to a UV screening effect which works in the opposite sense to the change in UV insolation. In both of these regimes, the signal from the stratospheric ozone could be obscured by the fluctuations in UV insolation. Figs. 1 and 2 show the detrended, deseasonalized data, both filtered and unfiltered, and the associated spectra for ozone and methane, respectively.

From the spectrum in Fig. 1(b), we can see that the dominant features of the ozone signal are two structures with periods of approximately 29 and 20 months. The 29 month period corresponds to the quasi-biennial oscilla-

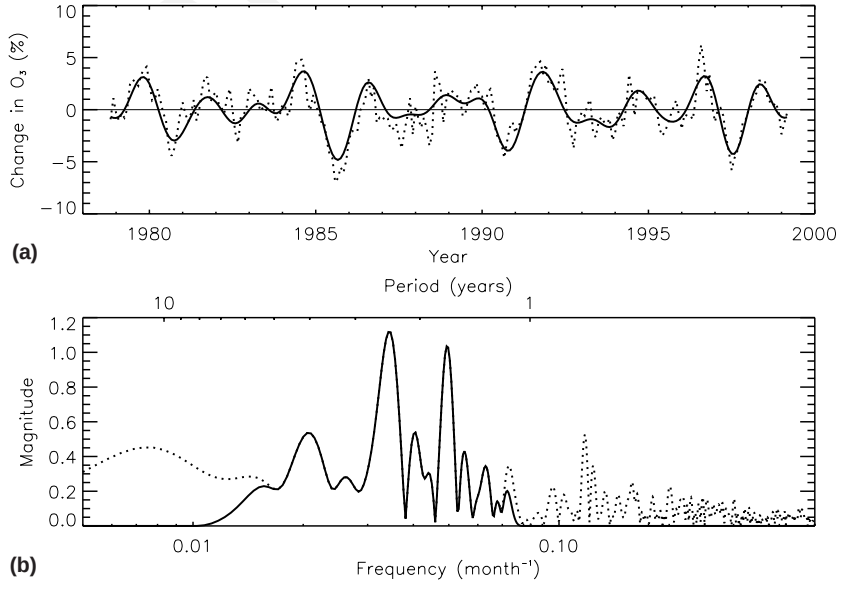

Fig. 1. (a) Fractional change in ozone column abundance from the merged SBUV/TOMS data set. (b) Spectrum of the ozone data. The solid line is the filtered data or spectrum and the dotted line is the unfiltered data or spectrum.

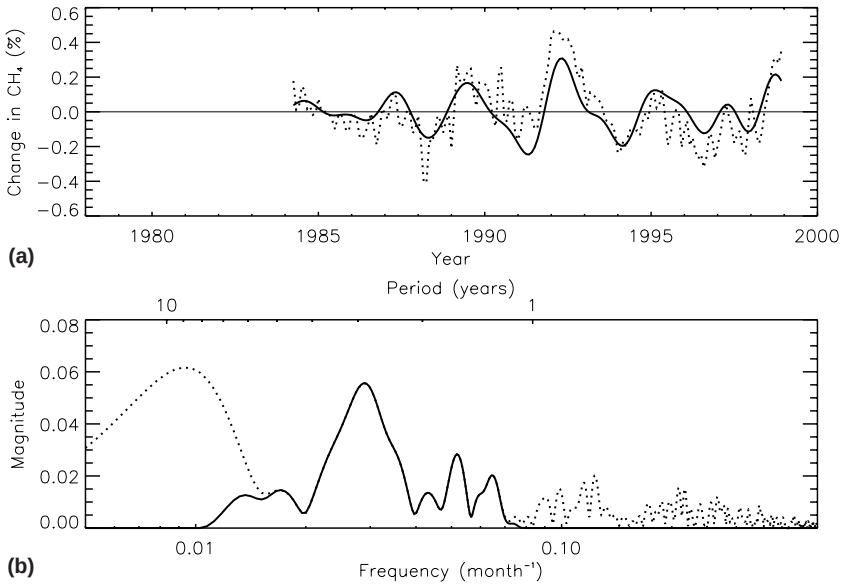

Fig. 2. (a) Fractional change in methane abundance from the NOAA-CMDL flask monthly means database. (b) Spectrum of the methane data. The solid line is the filtered data or spectrum and the dotted line is the unfiltered data or spectrum.

tion (QBO) of the stratosphere. The QBO is a quasi-periodic reversal in equatorial winds above the tropopause (Reed et al., 1961; Veryard and Ebdon, 1961). The presence of the signal in stratospheric ozone is well documented (Angell and Korshover, 1964, 1973; Tung and Yang, 1994). The QBO accounts for about 10% of total ozone variance. The 20 month signal is a beat frequency occurring from interactions between the QBO and annual fluctuations (Tung and Yang, 1994). Its frequency is the difference combination of the annual and QBO frequencies: $f_{\text{beat}} = f_{\text{annual}} - f_{\text{QBO}} = 1/12 - 1/29 \simeq 1/20$ months.

To determine the sensitivity, it is necessary to determine the delay of the methane response to the ozone forcing. We can estimate the delay directly from the data by calculating the cross correlation of the two data sets (truncated to their common time domain) for a range of lag times. The lag associated with the maximum correlation is the estimate of the delay. Fig. 3(a) shows that the delay is approximately 6 months. We can use our simple model, Eq. (8), to investigate this empirically determined value for the delay. If the forcing for this model is an oscillatory signal dominated by a single frequency and the lifetime, τ, is much longer than the period of the forcing, we expect the delay to be a quarter of the forcing period. This is derived in detail in SectionA.3 of Appendix A. From Fig. 1(b), we see that the period with the largest magnitude is the QBO, ~29 months. If the only dominant frequency in the forcing was that of the QBO, Eq. (A.9) shows that the delay would be ~7 months. On the other hand, if the only dominant frequency was that of the QBO-annual beat, with its ~20 month period, we would expect a delay of ~5 months. Since the ozone forcing is actually dominated by both the QBO and the QBO-annual beat, we expect a delay somewhere between these two values. This is clearly consistent with our empirically determined value of 6 months. The details of determining the delay for a signal consisting of the superposition of multiple periodic signals are examined in Section A.4 of Appendix A. If we estimate the delay using Eq. (A.16) for the two dominant frequencies of the ozone forcing, we recover a delay of ~6 months. This is illustrated in Fig. 3(b) which shows that the smallest positive root of $G(L) \equiv \cos(\omega_1 L) + \delta_2 \cos(\omega_2 L)$ is $L \simeq 6$. The frequencies, $\omega_1 \simeq 2\pi/29$ months^{-1} and $\omega_2 \simeq 2\pi/20$ months^{-1}, and amplitude ratio, $\delta_2 \simeq 1.0/1.1$, were determined from the filtered ozone spectrum shown in Fig. 1(b).

Once the appropriate delay of 6 months was determined, we created a paired data set consisting of the filtered ozone data for the interval from October 1983 to June, 1998 and the filtered methane data for the interval from April 1984 to December 1998. The sensitivity was then calculated by performing a least squares linear fit to the paired data, with α equal to the slope of the linear fit. Fig. 4 displays the paired data set and the linear fit. The results of the sensitivity calculations are given in Table 1. As expected from the definition of α, Eq. (5), the line from the linear fit passes close to the origin. The rather wide spread of the data will be discussed below. To get a very rough idea of the accuracy of alpha calculation, we have redone the calculation on a partition of the full

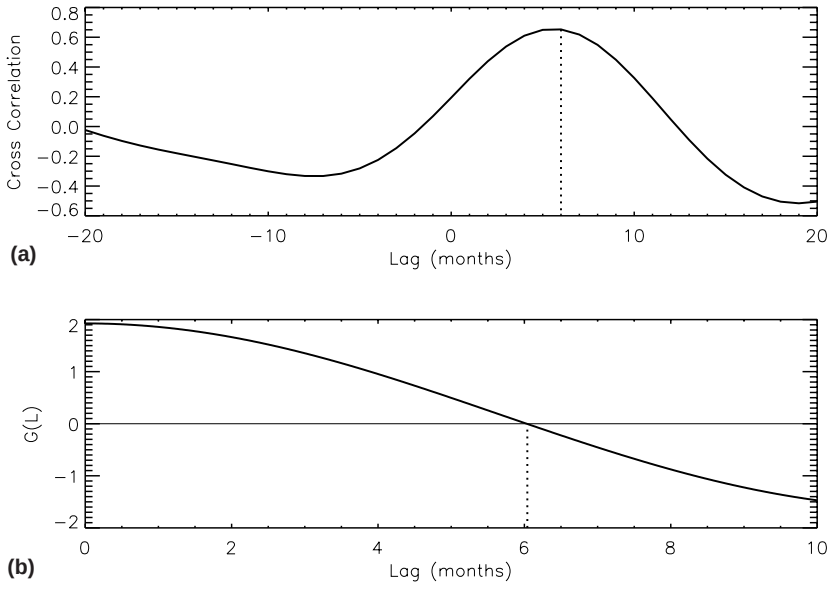

Fig. 3. Estimates of the delay of the methane response to the ozone forcing. (a) Cross correlation of the changes in ozone and methane abundances for the 1984–1998 period. The delay can be estimated by the lag corresponding to the maximum cross correlation. (b) Plot of $G(L)$ from Eq. (A.16). The delay can be estimated by the lag corresponding to the first positive root.

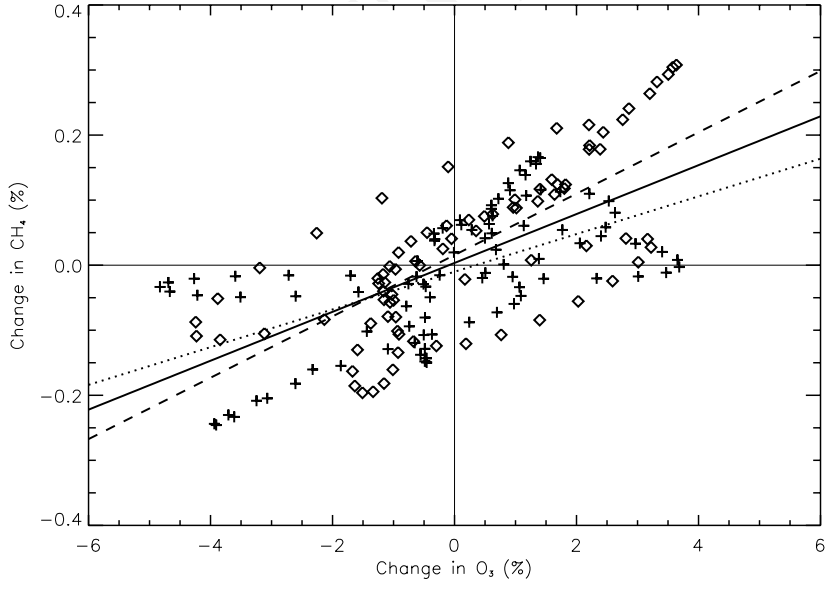

Fig. 4. Paired ozone – methane changes (with a 6 month delay). The sensitivity, α_{CH_4}, is the slope of the least squares linear fit (solid line) to the paired data. Data between April 1984 and December 1991 are denoted by +'s. Data between January 1992 and December 1998 are denoted by ◇'s. Least square linear fits are shown for the data prior to 1992 (dotted line) and the data for 1992 on (dashed line).

timeseries. The values of α (and the intercept) for data between 1984 and 1991 and for data between 1992 and 1998 are determined and shown in Table 1 and Fig. 4.

3. Simulating interannual fluctuations

To gain further insight into the effect of variability in stratospheric O_3 on tropospheric CH_4 and to test the

Table 1
Calculated sensitivity, α_{CH_4}, of the methane response to ozone fluctuations[a]

Years	Alpha	Intercept
1984–1998	−0.038	3.4×10^{-5}
1984–1991	−0.029	-1.0×10^{-4}
1992–1998	−0.047	1.6×10^{-4}

[a] The sensitivity is estimated by the slope of the linear fit to the paired ozone and methane data, as shown in Fig. 4. Values are shown for the entire time domain and for a partition of the time domain. Values for the intercepts of the linear fits are also given.

previously determined value for the sensitivity, α, Eq. (8) was integrated for the period from November 1978 to March 1999. The forcing used was

$$F(t) = -\alpha_{CH_4}\omega\tau\frac{\Omega'}{\Omega_0}, \tag{10}$$

where Ω'/Ω_0 is the filtered ozone data described in the previous section and shown in Fig. 1(a). The relationship between the sensitivity and the multiplicative factor for the forcing, $\kappa \simeq -\alpha_{CH_4}\omega\tau$, can be seen in Eq. (A.10). The change in sign is caused by the change from negative forcing by the hydroxyl radical to positive forcing by ozone. Values for the sensitivity, $\alpha_{CH_4} = -0.038$, and the QBO frequency, $\omega = 2\pi/29$ months^{-1}, were determined in the previous section. An estimate of 10 years has been used for τ, the lifetime of methane (Spivakovsky et al., 1990; Prinn et al., 1992; Michelson et al., 1994). The initial condition was set to zero and a fourth order Runge-Kutta method was used for the integration (Press et al., 1992c).

Fig. 5(a) shows the observed (filtered) ozone fluctuations in comparison to the observed (filtered) methane fluctuations. The ozone data has been multiplied by the sensitivity, α_{CH_4}, and has been shifted forward by 6 months to account for the delay in the methane response. Fig. 5(b) shows the resulting simulated methane response in comparison to the observed (filtered) methane data. The ozone signal and the simulation clearly capture much, but not all, of the variability of the methane signal. In particular, the phases of the oscillations are in reasonable agreement. The disparities between these curves will be discussed below. Correlations between the data sets have been calculated and are shown in Table 2. Corresponding statistical significances were determined by the Fisher-Z test. The necessary estimate of the number of degrees of freedom was found by using the first zero of the auto-correlation to estimate the spacing between independent data points (Harrison and Larkin, 1997).

4. Discussion

We can compare the estimate of α_{CH_4} from our empirical study to estimates of α_{OH} and α_{CH_4} from various modeling studies (Bekki et al., 1994; Fuglestvedt et al., 1994; Granier et al., 1996; Van Dop and Krol, 1996). Table 3, derived from Table 10.3 of (Granier and Shine, 1991), summarizes some of these results. But there exists

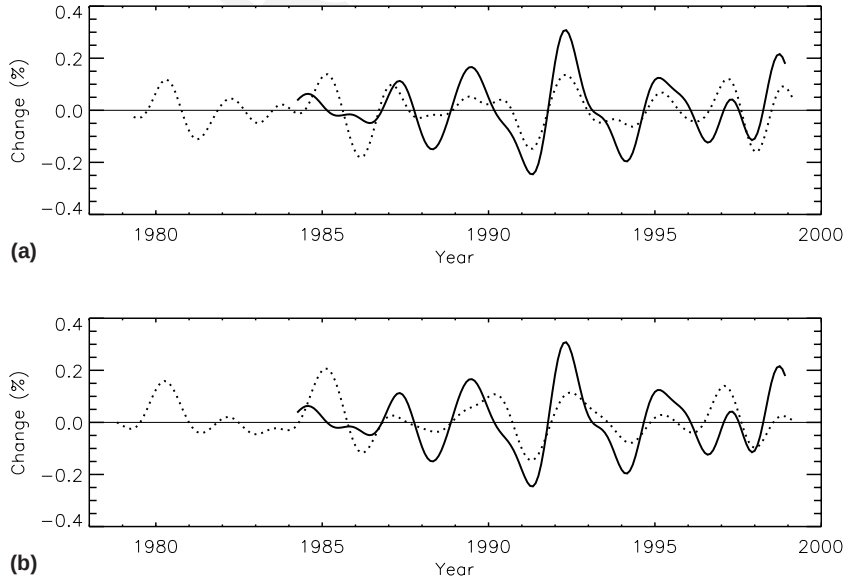

Fig. 5. (a) Comparison of the filtered methane data (solid line) to filtered ozone data (dashed line). The ozone data has been shifted up 6 months and its amplitude has been multiplied by the sensitivity, α_{CH_4}. (b) Comparison of the filtered methane data to the simulated methane response (dashed line).

Table 2
Correlations between the methane observations $(CH_4)_d$, and the ozone observations, O_3, and the simulated methane response, $(CH_4)_s$[a]

Data sets	Years	Correlations	R^2	Significance (%)	Degrees of freedom
$O_3 - (CH_4)_d$	1984–1998	0.65	0.43	99.99	26
$(CH_4)_s - (CH_4)_d$	1984–1998	0.53	0.29	99.6	23

[a] The coefficient of determination (R^2), associated Fisher Z significance and estimated degrees of freedom are also shown.

a fundamental difference between our time-dependent calculations and the steady-state ones performed in the modeling studies. Our calculations are based on the relatively short term response, on the order of months, to oscillatory forcing. The calculations from modeling studies are based on the long term response to a shift in the overall ozone level, i.e. to a constant forcing. The derivations in Sections A.2 and A.3 of Appendix A explore this difference for a simple linear system. For a species with a short lifetime, such as OH, Eqs. (A.5) and (A.8) demonstrate that the estimates of the sensitivity will not strongly depend upon whether the forcing is constant or oscillatory (assuming that forcing period, $2\pi/\omega$, is much longer than the lifetime, τ). However, for a long lifetime species such as CH_4, a comparison of Eqs. (A.5) and (A.10) demonstrates that the sensitivity measurement depends strongly on the type (and frequency) of the forcing. We can compare our empirical calculation of α_{CH_4} to the α_{CH_4} from Table 3 by including a multiplicative factor of $\omega\tau$. This also serves as a rough comparison of the empirical α_{CH_4} to the α_{OH}'s from Table 3. From Eqs. (4), (5), (A.8) and (A.10), we can estimate the ratio

$$\frac{\alpha_{CH_4}}{\alpha_{OH}} \simeq -\frac{1}{\omega\tau}. \tag{11}$$

Using $\alpha_{CH_4} \simeq -0.038 \pm 0.009$, $\omega = 2\pi/29$ months^{-1}, and $\tau = 10$ years, we get $\alpha_{CH_4}\omega\tau \simeq -0.98 \pm 0.23$. These values are consistent with the values from the modeling studies.

Table 3
Sensitivity, α_X, of tropospheric chemical species, X, to stratospheric ozone changes for the period 1979–1994[a]

References	X = OH	X = CH_4)
Bekki et al. (1994) (2-D)	0.86	N/A
Fuglestvedt et al. (1994) (2-D)	0.99	−0.79
Granier et al. (1996) (3-D)	0.82	N/A
Granier-1997 (3-D JPL94)	0.70	N/A
Granier-1997 (3-D JPL97)	0.74	N/A
Our result: $\alpha_{CH_4}\omega\tau$		−0.98

[a] The values reported here correspond to the relative change in global tropospheric annual average levels in X(%) resulting from a 1% decrease in total column ozone; the assumed scenarios are discussed in the cited publications. The type of model used is indicated in parentheses. Note that the values of Granier et al. (1996) correspond to the 1990–1994 period. The calculations indicated as Granier-1997 correspond to the 1979–1994 period and have been obtained using an updated version of the model used by Granier et al. (1996).

While the high significances of our correlations give us confidence that part of the methane signal is responding to the ozone forcing, the relatively low values of these correlations demonstrate that other processes have a strong effect on the methane on these timescales. The square of the correlation (the coefficient of determination or R^2) measures the amount of the variability in methane signal caused by the fluctuations in the ozone forcing. The R^2 values for our correlations, shown in Table 2, demonstrate that more than half of the methane variability is due to other causes. This is also evident in methane spectrum, Fig. 2(b), where the QBO and the QBO-annual beat frequencies are clearly not the dominant features. Other possible causes for the methane variability include source fluctuations and tropospheric dynamics. The signal from these other causes partially obscures the response to the local ozone forcing and contributes to the spread of the data used in the α calculation, Fig. 4, and to the disparities seen in the comparisons shown in Fig. 5. Investigating these effects is beyond the scope of the study presented here. A global study comparing measurements of the zonally averaged tropospheric methane from many latitude bands to measurements of the zonally averaged column ozone from each of those bands combined with a good measure of meridional mixing rates would be required.

We must also consider the possibility that there may exist alternative sources for our measured correlations. A process may be forcing both the ozone and methane directly, although it would need to affect the ozone approximately 6 months prior to the methane to explain the lag at which the maximum correlation occurs. One such alternative is that the QBO in the stratosphere may be directly creating a tropospheric QBO signal through dynamical processes. To explore this possibility, we examined the tropospheric CO_2 record from the CGO and MLO (Mauna Loa) sites. Since we detected no significant QBO signal in these records, we can rule out this hypothesis.

The signals we analyzed in this paper are very small, on the order of 0.1% for methane and 1.0% for ozone, over a few years. It is a tribute to the CMDL and TOMS programs that such high quality calibrations are maintained over decadal time periods. Obviously, this analysis can be greatly improved with a longer record in the future.

5. Uncited references

WMO (1961), Press et al. (1992b).

Acknowledgements

We thank M. Gerstell, P. Wennberg, J. Randerson, A. Ruzmaikin, A. Gould, J. Wang, R. Salawitch and an anonymous reviewer for helpful comments, E.J. Dlugokencky of NOAA-CMDL for the use of CH_4 data from the NOAA-CMDL global flask sampling network, and Rich Stolarski of NASA Goddard Space Flight Center for the use of O_3 data from the merged ozone data set. Supported by NASA grants NAG5-7230 and NAG1-1806 to the California Institute of Technology.

Appendix A

Our model is the first-order ODE

$$\frac{dy}{dt} = -\frac{1}{\tau}y - \frac{1}{\tau}F(t). \tag{A.1}$$

The general solution, given an initial condition $y(0)$ at time $t = 0$, is

$$y(t) = y(0)e^{-t/\tau} - \frac{1}{\tau}\int_0^t \exp\left[-\frac{1}{\tau}(t-t')\right]F(t')\,dt'. \tag{A.2}$$

A.1. Impulse response

If we assume that the forcing in Eq. (A.1) is an instantaneous impulse at some time t_0, i.e. $F(t) = \kappa\delta(t - t_0)$, then the solution (A.2) becomes

$$y(t) = \begin{cases} y(0)e^{-t/\tau} & \text{for } 0 < t < t_0, \\ y(0)e^{-t/\tau} - \frac{\kappa}{\tau}\exp[-\frac{1}{\tau}(t-t_0)] & \text{for } t > t_0. \end{cases} \tag{A.3}$$

Therefore, the solution responds immediately to the impulse forcing, then slowly decays back to $y = 0$. The speed of the decay is controlled by the lifetime, τ.

A.2. Constant forcing

If we assume that the forcing in Eq. (A.1) is constant, i.e. $F(t) = \kappa f(t) = \kappa f_0$, the solution (A.2) becomes

$$y(t) = [y(0) + \kappa f_0]e^{-t/\tau} - \kappa f_0. \tag{A.4}$$

Ignoring the transient terms, the sensitivity of the response to constant forcing can be estimated by

$$\alpha \simeq -\frac{\|y(t)\|}{f_0} \simeq \kappa. \tag{A.5}$$

Note that this result is independent of the lifetime, τ, of the responding species.

A.3. Single period oscillatory forcing

If we assume that the forcing in Eq. (A.1) is proportional to a sinusoidal forcing, i.e. $F(t) = \kappa f(t) = \kappa f_0\cos(\omega t)$, and define $\tan\phi = \omega\tau$, the solution (A.2) becomes

$$y(t) = [y(0) + \frac{\kappa f_0\cos(\phi)}{\sqrt{1+\omega^2\tau^2}}]e^{-t/\tau} - \frac{\kappa}{\sqrt{1+\omega^2\tau^2}}f_0 \times \cos(\omega t - \phi). \tag{A.6}$$

If we assume $\omega\tau \ll 1$, we get $\phi = \arctan(\omega\tau) \to 0$ and $\sqrt{1+\omega^2\tau^2} \simeq 1$. Ignoring the transient term, the solution (A.6) becomes

$$y(t) \simeq -\kappa f_0\cos(\omega t) \simeq -\kappa f(t). \tag{A.7}$$

So, the solution closely tracks the forcing. The sensitivity of the response of a short lifetime species to oscillatory forcing is estimated by

$$\alpha = -\frac{\|y(t)\|}{\|f(t)\|} = \frac{\kappa}{\sqrt{1+\omega^2\tau^2}} \simeq \kappa. \tag{A.8}$$

If we assume $\omega\tau \gg 1$, we get $\phi = \arctan(\omega\tau) \simeq \pi/2$ and $\sqrt{1+\omega^2\tau^2} \simeq \omega\tau$. Now the non-transient solution (A.6) becomes

$$y(t) \simeq -\frac{\kappa}{\sqrt{1+\omega^2\tau^2}}f_0\cos\left(\omega t - \frac{\pi}{2}\right) \simeq -\frac{\kappa}{\omega\tau}f\left(t - \frac{T}{4}\right), \tag{A.9}$$

where $T = 2\pi/\omega$ is the period of the forcing. So, for a long lifetime species, we get a response which lags the forcing by a quarter period. Furthermore, the sensitivity to oscillatory forcing can be estimated by

$$\alpha = -\frac{\|y(t)\|}{\|f(t)\|} = \frac{\kappa}{\sqrt{1+\omega^2\tau^2}} \simeq \frac{\kappa}{\omega\tau}. \tag{A.10}$$

A.4. Multiple period oscillatory forcing

For a more realistic forcing for Eq. (A.1), we can consider the superposition of multiple sinusoidal terms $F(t) = \kappa\sum_i f_i\cos(\omega_i t)$. Then, ignoring the transient terms, we get the solution

$$y(t) = -\kappa\sum_i \frac{f_i}{\omega_i\tau}\cos\left(\omega_i t - \frac{\pi}{2}\right). \tag{A.11}$$

When comparing datasets, the delay of the response to the forcing can be determined by finding the lag associated with the maximum (or minimum, if anti-correlated) cross-correlation between the two datasets. It would therefore be illuminating to examine the cross-correlation of the above idealized case. Note that here,

the solution and forcing are anti-correlated. The cross-correlation for the time interval $[0, T]$ is

$$\begin{aligned} C(y,F;L,T) &= \int_0^T y(t+L)F(t)\,\mathrm{d}t \\ &= \kappa \sum_i \sum_{j\neq i} \\ &\quad \times \frac{f_i f_j}{\omega_j \tau}\left[\frac{\cos[(\omega_j-\omega_i)T+\omega_j L]-\cos(\omega_j L)}{2(\omega_j-\omega_i)}\right. \\ &\quad \left.+\frac{\cos[(\omega_j+\omega_i)T+\omega_j L]-\cos(\omega_j L)}{2(\omega_j+\omega_i)}\right] \\ &\quad -\kappa\sum_i \frac{f_i^2}{\omega_i\tau}\left[\frac{T}{2}\sin(\omega_i L)\right. \\ &\quad \left.-\frac{\cos(2\omega_i T+\omega_i L)-\cos(\omega_i L)}{4\omega_i}\right]. \end{aligned} \tag{A.12}$$

We can greatly simplify this expression by letting T be the product of all possible periods in (A.12),

$$T=\prod_{i,j}(T_{ij+})(T_{ij-}), \qquad T_{ij\pm}=\frac{2\pi}{\omega_j\pm\omega_i} \tag{A.13}$$

leaving

$$C(y,F;L,T)=-\frac{\kappa T}{2}\sum_i \frac{f_i^2}{\omega_i\tau}\sin(\omega_i L). \tag{A.14}$$

The lag associated with the maximum anti-correlation occurs at the minimum of $C(y,F;L,T)$ with respect to L.

For a single forcing frequency, ω_1, the first minimum for positive lag, L, occurs when

$$\omega_1 L=\frac{\pi}{2}. \tag{A.15}$$

So the response lags the forcing by a quarter period as expected.

For two or more forcing frequencies, sorted by decreasing amplitude, the extrema occur at the roots of

$$G(L)\equiv\cos(\omega_1 L)+\sum_{i>1}\delta_i^2\cos(\omega_i L), \tag{A.16}$$

where $\delta_i = F_i/F_1 < 1$. If $\delta_i \ll 1$ for all $i > 1$, then this approximates the single frequency case with $\omega_i L = \pi/2 \pm \varepsilon$, $\varepsilon \ll 1$. In general, as the δ_i's grow, so will ε.

References

Angell, J., Korshover, J., 1964. Quasi-biennial variations in temperature, total ozone, and tropospheric height. Monthly Weather Review 101, 426–443.

Angell, J., Korshover, J., 1973. Quasi-biennial and long-term fluctuations in total ozone. Journal of the Atmospheric Sciences 21, 479–492.

Bekki, S., Law, K., Pyle, J., 1994. Effect of ozone depletion on atmospheric CH_4 and CO concentrations. Nature 371 (6498), 595–597.

Bojkov, R. Hudson, R., 1991. Ozone Variability and Trends. WMO, Section 4.2.1.

Dlugokencky, E., Lang, P. Masarie, K., Steele, L., 1997. Atmospheric methane mixing ratios – The NOAA/CMDL Global Cooperative Air Sampling Network, 1983–1993. Technical Report, Carbon Dioxide Information Analysis Center.

Fuglestvedt, J., Jonson, J., Isaksen, I., 1994. Effects of reductions in stratospheric ozone on tropospheric chemistry through changes in photolysis rates. Tellus Series B-Chemical and Physical Meteorology 46 (3), 172–192.

Granier, C., Müller, J., Madronich, S., Brasseur, G., 1996. Possible causes for the 1990–1993 decrease in the global tropospheric CO abundances: a three-dimensional sensitivity study. Atmospheric Environment 30 (10-11), 1673–1682.

Granier, C., Shine, K., 1991. Climate Effects of Ozone and Halocarbon Changes. WMO (Chapter 10).

Harrison, D., Larkin, N., 1997. Darwin sea level pressure, 1876–1996: evidence for climate change? Geophysical Research Letters 24 (14), 1779–1782.

Khalil, M., Shearer, M., Rasmussen, R., 1993. Methane sinks and distribution. In: Khalil, M. (Ed.), Atmospheric Methane: sources, sinks, and role in global change, Vol. 13 of NATO ASI series. Series I, Global Environmental Change. Springer, Berlin, New York, published in cooperation with NATO Scientific Affairs Division; Proceedings of the NATO Advanced Research Workshop on the Atmospheric Methane Cycle: Sources, Sinks, Distributions, and Role in Global Change, held at Mt. Hood near Portland, OR, USA, 7–11 October 1991.

Levy, H., 1992. Photochemistry of the lower troposphere. Planetary and Space Science 20, 919–935.

Liu, S., Tranier, M., 1988. Responses of the tropospheric ozone and odd hydrogen radicals to column ozone changes. Journal of Atmospheric Chemistry 6 (3), 221–233.

McPeters, R., Bhartia, P., Krueger, A., Herman, J., Schlesinger, B., Wellemeyer, C. Seftor, C., Jaross, G., Taylor, S., Swissler, T., Torres, O., Labow, G., Byerly, W., Cebula, R., 1996. Nimbus-7 Total Ozone Mapping Spectrometer (TOMS) data products user's guide. Technical Report, NASA.

Michelson, H., Salawitch, R., Wennberg, P., Anderson, J., 1994. Production of $O(^1D)$ from photolysis of O_3. Geophysical Research Letters 21 (20), 2227–2230.

Press, W., Teukolsky, S., Vetterling, W., Flannery, B., 1992a. In: Press et al. (Eds.), Fourier and Spectral Methods, 1992b, pp. 530–602 (Chapter 13).

Press, W., Teukolsky, S., Vetterling, W., Flannery, B., 1992b. Numerical Recipes in Fortran 77: The Art of Scientific Computing, second ed. Cambridge University Press, Cambridge.

Press,W., Teukolsky, S., Vetterling, W., Flannery, B., 1992c. In: Press et al. (Eds.) Runge–Kutta Method, Section 16.1, 1992b, pp.704–708.

Prinn, R., Cunnold, D., Simmonds, P., Alyea, F., Boldi, R., Crawford, A., Fraser, P., Gutzler, D., Hartley, D., Rosen, R., Rasmussen, R., 1992. Global average concentration

and trend for hydroxyl radicals deduced from ALE-GAGE trichloroethane (methyl chloroform) data for 1978–1990. Journal of Geophysical Research-Atmospheres 97(D2), 2445–2461.

Reed, R., Campbell, W., Rasmussen, L., Rogers, D., 1961. Evidence of downward-propagating annual wind reversal in the equatorial stratosphere. Journal of Geophysical Research 66, 813–818.

Spivakovsky, C., Yevich, R., Logan, J., Wofsy, S., McElroy, M., Prather, M., 1990. Tropospheric OH in a 3-dimensional chemical tracer model – an assessment based on observations of CH_3CCl_3. Journal of Geophysical Research-Atmospheres 95 (D11), 18441–18471.

Thompson, A., 1992. The oxidizing capacity of the Earth's atmosphere – probable past and future changes. Science 256 (5060), 1157–1165.

Tung, K., Yang, H., 1994. Global QBO in circulation and ozone. Part I: reexamination of observational evidence. Journal of the Atmospheric Sciences 51 (19), 2699–2707.

Dop, H., Krol, M., 1996. Changing trends in tropospheric methane and carbon monoxide: a sensitivity analysis of the OH-radical. Journal of Atmospheric Chemistry 25 (3), 271–288.

Veryard, R., Ebdon, R., 1961. Fluctuations in tropical stratospheric winds. Meteorological Magazine 90, 125–134.

WMO, 1991. Scientific Assesment of Ozone Depletion: 1998. World Meteorological Organization: Global Ozone Research and Monitoring Project – Report No. 44.